

# Photosensitization with Zinc (II) Phthalocyanine as a Switch in the Decision between Apoptosis and Necrosis<sup>1</sup>

Clara Fabris, Giuliana Valduga, Giovanni Miotto, Lara Borsetto, Giulio Jori, Spiridione Garbisa,<sup>2</sup> and Elena Reddi

Departments of Biology [C. F., G. V., L. B., G. J., E. R.], Biological Chemistry [G. M.], and Experimental Biomedical Sciences [S. G.], The University of Padova, I-35131 Padova, Italy

## ABSTRACT

Photodynamic therapy (PDT) of tumors and other diseases is based on the uptake of a photosensitizing dye in target cells, which are damaged by reactive oxygen intermediates generated on irradiation with light in which the wavelengths match the dye absorption spectrum. PDT can induce cell death by necrosis and apoptosis both *in vivo* and *in vitro*, but the factors determining the contribution of either mechanism to the overall process are not completely defined. Our studies on the photosensitization of 4R transformed fibroblasts with the second-generation photosensitizer zinc (II) phthalocyanine (ZnPc) aim at determining the effect of important experimental parameters such as time of cell incubation (2 or 24 h) with ZnPc before irradiation and ZnPc concentration in the incubation medium on cell death. Furthermore, we propose possible correlations between the cell death mechanism and primary photo-damage sites; these are mainly determined by the intracellular localization of the photosensitizer. The mechanism of cell death was determined by both electron microscopy analysis of the morphological alterations induced by photosensitization and measurement of caspase 3 activation. The initial photo-damage sites were determined by measuring the activities of several functions typical of mitochondria, lysosomes, Golgi apparatus, cytosol, and plasma membrane. The intracellular localization of ZnPc after 2- or 24-h incubation was determined by fluorescence microscopy. Necrosis, associated with early loss of plasma membrane integrity and complete depletion of intracellular ATP, represents the prevailing mode of death for 4R cells dark-incubated for 2 h with ZnPc and irradiated with light doses reducing viability by 99.9%. In contrast, irradiation performed 24 h after ZnPc incubation causes only partial inhibition of plasma membrane activities, and cell death occurs largely by apoptosis. ZnPc is mainly localized in the Golgi apparatus after 2- and 24-h incubation, and in all of the cases this compartment represents a primary target of photodamage. Only after prolonged incubation is mitochondrial localization of ZnPc clearly detected by fluorescence microscopy; this could be a determining factor for promotion of apoptosis. Our data demonstrate that it is possible to modulate the mechanism of cell death by appropriate protocols; this may be relevant for enhancing the therapeutic efficacy of PDT.

## INTRODUCTION

PDT<sup>3</sup> is a viable treatment modality for a variety of tumors as well as for selected nononcological diseases (1–3). At present, PDT with Photofrin as a phototherapeutic agent has been approved for clinical use in an increasing number of countries (4). At the same time, new photosensitizers with improved spectroscopic, photochemical, and tumor-localizing properties are being tested, which expand the scope of tumor PDT and stimulate clinical applications outside the oncological field (5, 6). All of the photosensitizers studied thus far induce cell/tissue photodamage through the production of reactive cytotoxic

species, mainly singlet oxygen, which have a short lifetime in biological systems and, consequently, a radius of action shorter than 0.02  $\mu\text{m}$  (7). This implies that the initial cell damage sites are very close to those of singlet oxygen formation and strictly related to the distribution of the sensitizer in the cell. The latter is determined by both the physicochemical characteristics of the photosensitizer (8) and the protocol adopted for its incubation with the cells before light exposure. Consequently, the loss of cell viability may occur with a very different efficiency when using PDT sensitizers that produce cytotoxic species with comparable quantum yields but localize in fairly vulnerable cellular sites.

PDT can induce cell death through necrosis or apoptosis both *in vitro* and *in vivo* (9). Apoptosis is an intrinsic physiological event, which can also be triggered by external stimuli like oxidative stress attributable to photosensitization. An apoptotic response was observed in a variety of tumor cell lines after photosensitization with different porphyrin and phthalocyanine derivatives (10–12). However, the factors controlling the mechanism of PDT-induced cell death have not yet been completely defined.

The unsubstituted lipophilic ZnPc selected for our studies is a second-generation photosensitizer that efficiently localizes in experimental tumors *in vivo* and, after irradiation, causes regression of the neoplastic lesion by inducing both necrosis and apoptosis (13, 14). *In vitro*, low ZnPc concentrations (1  $\mu\text{M}$ ) photosensitize to death various types of transformed cells with high efficiency (15, 16).

In the present investigation we extend our studies to cell photosensitization with ZnPc with the aim of determining whether necrosis or apoptosis is the prevailing mechanism of cell death. Furthermore, we attempt to establish whether there is any correlation between cell death mode and the sites of initial photodamage. Because the latter are largely determined by the subcellular localization of ZnPc, which may be affected by incubation time, we performed our investigations under different incubation protocols before irradiation.

## MATERIALS AND METHODS

**Chemicals.** The liposomal formulation of ZnPc was supplied by Ciba-Geigy (Basel, Switzerland) in freeze-dried form and rehydrated by addition of water before use (13, 17). Radioactively labeled thymidine (methyl-<sup>3</sup>H], 0.15 mM solution with a specific activity of 6.7 Ci/mmol), AIB ([1-<sup>14</sup>C], 2 mM solution with a specific activity of 51 mCi/mmol), valine (L[1-<sup>14</sup>C], 0.35 mM solution with a specific activity of 283 mCi/mmol), and deoxyglucose (<sup>3</sup>H(G)], 0.1 mM solution with a specific activity of 10 Ci/mmol) were purchased from DuPont (Brussels, Belgium). Uridine diphospho-D-[6-<sup>3</sup>H] galactose (0.21 mM solution) with a specific activity of 4.7 Ci/mmol was purchased from Amersham Life.

**Cell Line.** The transformed rat embryo fibroblast cell line 4R was used (18, 19). The cells cultured in monolayer at 37°C in a humidified atmosphere with 5% CO<sub>2</sub> were grown in DMEM (Sigma Chemical Co.) containing 10% heat-inactivated FCS and supplemented with 100 units/ml penicillin, 100  $\mu\text{g}/\text{ml}$  streptomycin, 0.25  $\mu\text{g}/\text{ml}$  amphotericin, and 2 mM glutamine (Sigma Chemical Co.).

**Cell Phototoxicity Experiments.** 4R cells were seeded in Petri dishes (60-mm diameter) at a density of 20,000 cells/cm<sup>2</sup> and grown for 20 h in DMEM with 10% FCS. The growth medium was removed, replaced with DMEM without or with 3% FCS at the desired ZnPc concentration (0.4 or 1

Received 2/14/01; accepted 8/9/01.

The costs of publication of this article were defrayed in part by the payment of page charges. This article must therefore be hereby marked *advertisement* in accordance with 18 U.S.C. Section 1734 solely to indicate this fact.

<sup>1</sup> Supported by the Ministero dell'Università e Ricerca Scientifica e Tecnologica and Associazione per la Ricerca sul Cancro.

<sup>2</sup> To whom requests for reprints should be addressed, at Department of Experimental Biomedical Sciences, via G. Colombo 3, I-35121 Padova, Italy. Phone: 39-049-8276088; Fax: 39-049-8276089; E-mail: garbisa@civ.bio.unipd.it.

<sup>3</sup> The abbreviations used are: PDT, photodynamic therapy; AIB,  $\alpha$ -aminoisobutyric acid; R123, rhodamine-123; TCA, trichloroacetic acid; ZnPc, zinc (II) phthalocyanine; HClO<sub>4</sub>, perchloric acid.

$\mu\text{M}$ ), and the cells incubated at  $37^\circ\text{C}$  for 2 or 24 h, respectively. After incubation, the ZnPc-containing medium was removed, the cells were washed twice with 2 ml of PBS containing  $\text{Ca}^{2+}$  and  $\text{Mg}^{2+}$  and irradiated in the same buffer for various periods of time with red light (585–605 nm) from a 250 W slide projector lamp. The light fluence rate on the cell monolayer was 1.5 or 10  $\text{mW}/\text{cm}^2$ . The effect on cell survival of ZnPc alone, light alone, and ZnPc in combination with light was evaluated by the clonogenic assay (15).

**Enzyme Activity Assays.** The effect of PDT on the activity of enzymes located in different cellular compartments was evaluated immediately after cell treatment.

The activity of NADH dehydrogenase and lactate dehydrogenase was measured in cell lysates prepared as described by Valduga *et al.* (15) and following the procedures described by Galante and Hatefi (20) and by Reeves and Fimognari (21). The *N*-acetyl- $\beta$ -glucosaminidase activity was measured following Beaufay *et al.* (22) and modified as described by Valduga *et al.* (15). In each cell lysate, the protein concentration was measured by the bicinchoninic acid assay (23).

The UDP galactosyl transferase activity was measured as described by Brandli *et al.* (24). The activity of this enzyme is evaluated as its ability to bind the radioactive-labeled uridine diphospho-galactose to ovalbumin and is monitored by scintillation counting of the radioactivity in the TCA insoluble fraction of the cell material.

**Cellular Uptake of [ $^{14}\text{C}$ ]Valine.** Immediately after treatment, the cells were incubated for 3 min or 30 min at  $37^\circ\text{C}$  with 1.75  $\mu\text{M}$  (0.5  $\mu\text{Ci}/\text{ml}$ ) [ $^{14}\text{C}$ ]valine in PBS containing  $\text{Ca}^{2+}$  and  $\text{Mg}^{2+}$  for measuring the transport of the amino acid through the plasma membrane and incorporation into proteins (25). After incubation, the cell monolayer was washed twice with cold PBS, and 2 ml of 10%  $\text{HClO}_4$  was added. The incorporation of [ $^{14}\text{C}$ ]valine in the  $\text{HClO}_4$ -soluble and -insoluble fraction was measured by scintillation counting.

**Transport of Thymidine, Deoxyglucose, and AIB.** The transport of thymidine was measured immediately after irradiation by incubating the cells with DMEM containing 10% FCS and 0.15  $\mu\text{M}$  [ $^3\text{H}$ ]thymidine for 1 min. The cell layer was washed twice with cold PBS containing  $\text{Ca}^{2+}$  and  $\text{Mg}^{2+}$ , and the thymidine incorporated into the cells was extracted after 15 min incubation with 5% TCA on ice. The radioactivity of the TCA-soluble fraction was measured by scintillation counting. The transport of deoxyglucose and AIB into cells was measured after incubation of the cell monolayers with 0.1  $\mu\text{M}$  of [ $^3\text{H}$ ]deoxyglucose and 2  $\mu\text{M}$  [ $^{14}\text{C}$ ]AIB in PBS containing  $\text{Ca}^{2+}$  and  $\text{Mg}^{2+}$  for 10 and 20 min. After three washing steps with cold PBS, the cells were solubilized with 2% SDS and radioactivity measured.

**Determination of ATP Content.** ATP levels were measured in the treated and untreated cells. ATP was extracted from the cells after incubation for 10 min on ice with 8%  $\text{HClO}_4$ . The extract was neutralized with 2 M  $\text{KOH}$ -1 M  $\text{NaHCO}_3$  solution, and after centrifugation for 15 min at  $2,500 \times g$ , the ATP content in the supernatant was determined using the Bioluminescence CLS kit (Boehringer Mannheim, Mannheim, Germany) and an LKB luminometer (Bromma, Stockholm, Sweden).

**Caspase 3 Activity.** The activity of caspase 3 was measured in the PDT-treated cells at various post-treatment times. The ApoAlert CPP32 kit (Clontech, Palo Alto, CA) was used. According to manufacturer-recommended procedure,  $10^6$  cells were collected by centrifugation, resuspended in 50  $\mu\text{l}$  of lysis buffer, and held for 10 min on ice. Then, 50  $\mu\text{l}$  of reaction buffer containing DTT and 5  $\mu\text{l}$  of DEVD-7-amino-4-trifluoromethyl coumarin were added to the cell lysate, and after 1 h incubation at  $37^\circ\text{C}$ , the fluorescence emitted at 505 nm ( $\lambda_{\text{ex}} = 400 \text{ nm}$ ) was measured with a Perkin-Elmer LS50 spectrofluorometer. The caspase 3 activity in the treated cells was expressed as fold increase of the emitted fluorescence, taking the fluorescence from untreated cells as reference.

**Electron Microscopy.** At predetermined times after PDT treatment, the cells were trypsinized, collected by centrifugation, fixed with 2% glutaraldehyde in 0.1 M phosphate buffer (pH 7.2), and post-fixed with 1%  $\text{OsO}_4$ . Dehydration was performed in a graded series of ethanol solutions followed by embedding in Epon. The cells were microsectioned, stained with uranyl acetate and lead citrate, and observed in a Hitachi H-600 transmission electron microscope.

**Fluorescence Microscopy.** The intracellular localization of ZnPc after incubation of 2 and 24 h was determined with an Olympus IMT-2 fluorescence microscope equipped with a refrigerated CCD camera (Micromax; Princeton Instruments). A 75-W xenon lamp was used as the excitation source. Fluores-

cence images obtained with a  $60\times 1.4 \text{ NA}$  oil immersion objective (Olympus) were acquired and analyzed with the imaging software Metamorph (Universal Imaging). The cellular distribution of ZnPc fluorescence was compared with that of R123 and NBD [ $\text{C}_6$ ]ceramide (Molecular Probes, Leiden, Netherlands), used as markers for the mitochondria and Golgi apparatus, respectively. Appropriate excitation and emission cubes (Chroma Technology Corp.) were used for the fluorescent dyes: 616/770 nm for ZnPc and 475/520 nm for R123 and NBD [ $\text{C}_6$ ]ceramide.

## RESULTS

**Cytotoxic Effect of ZnPc and Light.** 4R cells dark-incubated for 24 h with 0.4 or 1  $\mu\text{M}$  of ZnPc underwent almost complete cell killing ( $\sim 99.9\%$ ) after 2–3 min of exposure to red light at a fluence rate of 1.5  $\text{mW}/\text{cm}^2$  (Fig. 1). The efficiency of cell photoinactivation was modestly influenced by the phthalocyanine concentration despite the almost double accumulation of ZnPc in the cells exposed to 1  $\mu\text{M}$  compared with a 0.4- $\mu\text{M}$  concentration ( $0.37 \pm 0.04$  and  $0.2 \pm 0.03$  nmol ZnPc/mg cell proteins; Ref. 17).

**Intracellular Localization of ZnPc.** Fluorescence microscopy showed that 4R cells incubated 2 h with 1  $\mu\text{M}$  of ZnPc exhibited red fluorescence typical of ZnPc and mainly localized in a cytoplasmic region (Fig. 2A). The fluorescent probe for the Golgi apparatus NBD [ $\text{C}_6$ ]ceramide was also colocalized here (Fig. 2B), as shown by the yellow fluorescence observed when the two fluorescence images were superimposed (Fig. 2C). The ZnPc fluorescence was very weak in cytoplasmic regions outside the Golgi apparatus, and localization in the plasma membrane or colocalization with the mitochondrial probe R123 were not evident. When incubation was prolonged to 24 h, the ZnPc fluorescence in the Golgi apparatus intensified and a speckled, less intense red fluorescence was observed throughout the cytoplasm (Fig. 2D). In particular, ZnPc was partially colocalized with R123, suggesting a relatively high concentration of ZnPc accumulated by mitochondria after a 24-h incubation (Fig. 2, E and F).

**Cellular Targets of ZnPc Photosensitization.** Enzyme activity measurements showed that in cells incubated 24 h with 1  $\mu\text{M}$  of ZnPc, the lysosomal enzyme *N*-acetyl- $\beta$ -glucosaminidase was not affected by photosensitization, because its activity was fully preserved also in cells undergoing 99.9% death. Under the same irradiation conditions, mitochondrial NADH dehydrogenase and cytosolic lactate dehydrogenase activity was reduced to  $51.9 \pm 6.9\%$  and  $76.8 \pm 20.4\%$  of the activity of untreated controls, respectively.

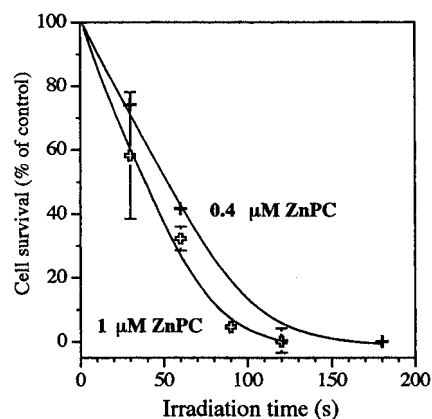


Fig. 1. Survival of 4R cells irradiated for different periods of time after dark-incubation with ZnPc. 4R cells were incubated for 24 h with 0.4 or 1  $\mu\text{M}$  of ZnPc in DMEM supplemented with 3% FCS, washed twice with PBS, and irradiated in PBS with red light at a fluence rate of 1.5  $\text{mW}/\text{cm}^2$  for different periods of time. After phototreatment, the cells were incubated at  $37^\circ\text{C}$  in a medium containing 10% FCS, 45% DMEM, and 45% medium from subconfluent cultures, and survival was evaluated by the clonogenic assay. Each data point represents the mean from at least three separate experiments; bars,  $\pm$  SD.

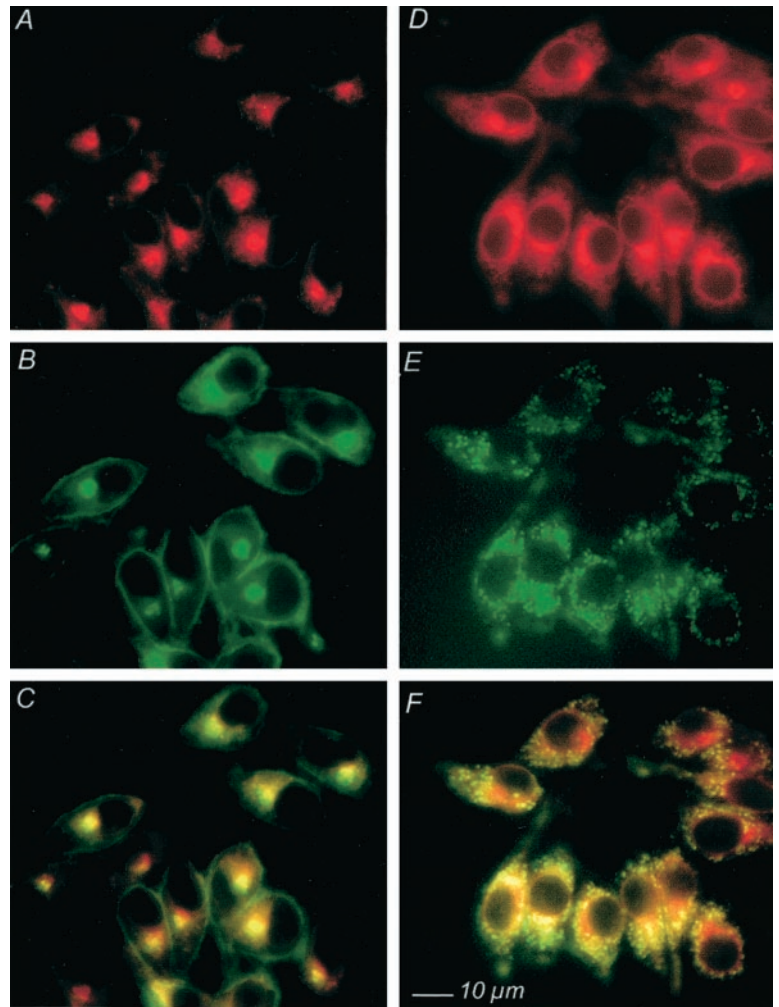


Fig. 2. Intracellular localization of 1  $\mu\text{M}$  of ZnPc in 4R cells after incubation for 2 or 24 h. After 2-h incubation the red fluorescence of ZnPc (A) is mainly colocalized with the green fluorescence of NBD [C<sub>6</sub>]-ceramide (B) as shown by the yellow fluorescence of the superimposed images (C). After 24-h incubation the red fluorescence of ZnPc (D) shows a partial colocalization with the R123 fluorescence (E) as shown in the superimposed fluorescence images (F).

The activity of the UDP galactosyl transferase in the Golgi apparatus was completely inhibited in cells dark-incubated with 1  $\mu\text{M}$  of ZnPc for 2 or 24 h and irradiated with light doses yielding similar percentages of cell killing. In both cases complete inhibition of this enzyme was observed even in cells treated with light doses causing only ~60% cell mortality.

The activity of several transport proteins of the plasma membrane was affected to a different extent by ZnPc photosensitization. The transport of thymidine was 80% inhibited in cells undergoing complete killing, whereas AIB transport was inhibited only 35% (Fig. 3). 4R cells incubated for 24 h with 1 or 0.4  $\mu\text{M}$  of ZnPc and irradiated with increasing doses of light causing up to 99.9% cell killing showed reduction of deoxyglucose uptake to ~20 and 70%, respectively (Fig. 4A). The inhibition of deoxyglucose uptake seems to be correlated with the depletion of cellular ATP (Fig. 4B). In cells irradiated after incubation with 1  $\mu\text{M}$  of ZnPc, the ATP level was reduced to 10–20% of the control whereas only ~50% reduction was observed in cells exposed to 0.4  $\mu\text{M}$  of ZnPc.

On the other hand, only irradiation performed after 2-h incubation with 1  $\mu\text{M}$  of ZnPc caused notable reduction of valine uptake into the cells, whereas valine transport was inhibited by no more than 40% after irradiation performed at 24 h (Fig. 5). However, incorporation of valine into proteins was drastically inhibited by both photosensitization protocols and approached zero also after irradiation causing modest cell mortality (Fig. 5).

In all of the cases the selected functions were not affected by

incubation of 4R cells with ZnPc in the dark or by cell irradiation in the absence of ZnPc.

**Mode of Cell Death: Necrosis versus Apoptosis.** The morphological changes occurring in 4R cells undergoing 99.9% killing after 2-h

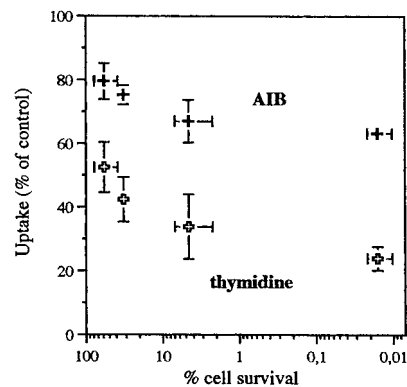


Fig. 3. Inhibition of the transport of thymidine and AIB as a function of the survival of 4R cells photosensitized with ZnPc. 4R cells were incubated for 24 h with 1  $\mu\text{M}$  of ZnPc and irradiated after washing and replacement of the ZnPc-containing medium with PBS as described in Fig. 1. Immediately after irradiation the cells were exposed to 0.15  $\mu\text{M}$  of [<sup>3</sup>H]thymidine for 1 min or 2  $\mu\text{M}$  [<sup>14</sup>C]AIB for 20 min. The amount of thymidine and AIB transported into the cells was measured by scintillation counting as described in "Materials and Methods." The uptake relative to the untreated control cells is reported as a function of cell survival measured under the same experimental conditions. The data represent the mean of at least three separate experiments; bars,  $\pm$  SD.



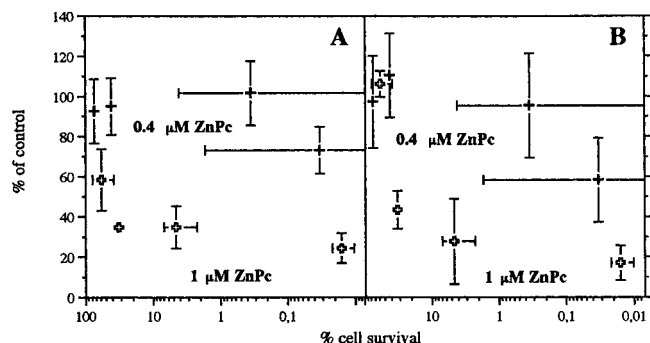


Fig. 4. Inhibition of deoxyglucose uptake (A) and ATP levels (B) in 4R cells after ZnPc photosensitization. 4R cells dark-incubated for 24 h with 0.4 or 1 μM of ZnPc were irradiated as described in Fig. 1. A, immediately after irradiation the cell monolayers were exposed to 0.1 μM of [<sup>3</sup>H]deoxyglucose for 10 min, washed, and lysed with 2% SDS before the radioactivity measurements. The uptake of deoxyglucose relative to untreated cells is reported as a function of cell survival measured after photosensitization under the same conditions (see Fig. 1). B, immediately after phototreatment ATP was extracted from the cells and measured by the bioluminescence method. The ATP levels in the treated cells are calculated relative to untreated controls and reported as a function of cell survival. Each data point represents the mean of three separate determinations; bars, ± SD.

incubation with 1 μM of ZnPc included a pronounced vacuolization of the cytoplasm already at 3 h after PDT (Fig. 6D), which evolved to profound alterations of all of the cytoplasmic organelles and the plasma membrane at 6 h (Fig. 6E). These effects eventually led to cell lysis typical of necrotic cell death. In cell monolayers irradiated with light dose yielding 50% survival, only a fraction of the damaged cells showed alterations similar to those described above (Fig. 6B); some cells exhibited perinuclear chromatin condensation and fragmentation with the formation of apoptotic bodies containing condensed chromatin (Fig. 6C). The observations suggest induction of both necrotic and apoptotic cell death.

In contrast, the 24 h-incubated cells that underwent a 99.9% killing predominantly exhibited morphological alterations typical of apoptosis including chromatin condensation on the nuclear envelope at 3 h after PDT (Fig. 6F), followed by nuclear fragmentation (Fig. 6G) at 6 h after PDT. In cells exhibiting morphological changes typical of the apoptotic process, significant activation of caspase 3 was found (see Fig. 7, B and C). This did not depend on the ZnPc concentration (0.4 or 1 μM) used to obtain 99.9% cell killing and was observed with light doses yielding 50 and 99.9% cell killing (Fig. 7B). However, cells irradiated after 2-h incubation with ZnPc showed a significant activation of caspase 3 only with light doses inducing 50% mortality (Fig. 7A).

DISCUSSION

Photosensitivity dose- and time-response results indicate a different localization of ZnPc within 4R transformed fibroblasts. In fact, a nonsignificant difference was observed on the survival of the cells photosensitized with different ZnPc concentrations (0.4 and 1 μM) for up to 24 h (Fig. 1). Furthermore, when the cells were allowed to accumulate the same level of ZnPc over a 2 or 24 h period, a 6-fold lower light dose was required to induce complete killing of the cells with the longer incubation. In the cells incubated for the shorter period, fluorescence microscopy showed that ZnPc was mainly localized in the Golgi apparatus, and the complete inhibition of the UDP galactosyl transferase activity confirmed the Golgi apparatus represents an important target of ZnPc photosensitization. Protein synthesis was drastically inhibited as well (Fig. 5), but whether this was caused by direct damage to endoplasmic reticulum or a consequence of impairment of the transport of several biomolecules, including deoxyglucose, AIB, thymidine (15), and valine (Fig. 5), demonstrated that the plasma membrane represents an additional important target. This was confirmed by positive trypan blue staining of >90% of the cells within 30 min of irradiation. It is likely that ZnPc levels in the plasma membrane are too low for clear fluorescence microscopy detection but are sufficiently high to induce complete inhibition of the activity of several transporters. In cells irradiated after 24-h incubation, the same transport activities were inhibited to a smaller extent (Figs. 3–5). The lower inhibition of the transport activities may be attributable to either migration of ZnPc from the plasma membrane toward inner cellular sites or the lower light dose required for inducing almost complete cell mortality. The fluorescence microscopy images of cells incubated for 24 h showed that ZnPc was still present in the Golgi apparatus, but a mitochondrial localization could be clearly observed as well. However, the mitochondrial localization of ZnPc also led to only partial (51.9 ± 6.9%) inhibition of NADH dehydrogenase in cells undergoing almost complete killing. The NADH dehydrogenase activity was also inhibited to a similar extent in 4R cells irradiated after 2-h incubation in which fluorescence microscopy did not give clear revelation of mitochondrial localization of ZnPc (15). An ~50% inhibition of activity was reported also for cytochrome c oxidase in NHIK 3025 carcinoma cells exposed for 18 h to ZnPc and irradiated with light doses inducing >90% loss of viability (16). Thus, it appears that the ZnPc concentration in mitochondria does not correlate with the extent of inhibition of some components of the respiratory chain. It is likely that most of the ZnPc

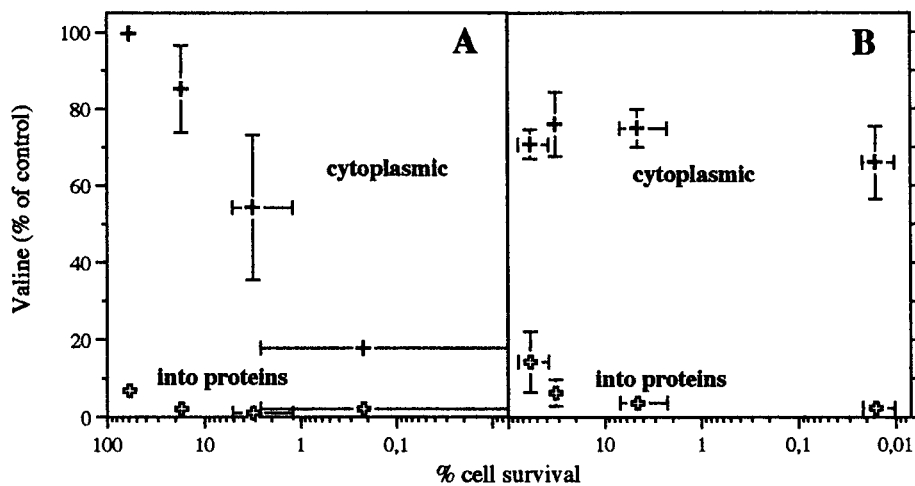


Fig. 5. Inhibition of the valine transport and protein synthesis in 4R cells photosensitized with ZnPc. A, 4R cells were incubated for 2 h with 1 μM of ZnPc, washed, and irradiated in PBS with red light at a fluence rate of 10 mW/cm<sup>2</sup> for 0.5–3 min. After irradiation the cell monolayers were exposed to 1.75 μM [<sup>14</sup>C]valine for 3 min or 30 min, respectively, for the measurements of valine transport or protein synthesis. B, 4R cells were incubated for 24 h with 1 μM of ZnPc, irradiated with a fluence rate of 1.5 mW/cm<sup>2</sup>, and then processed as in A. The amount of valine transported into the cells or incorporated into proteins relative to untreated cells is reported as a function of the cell survival measured under the same experimental conditions. The values of cell survival used in the plot of A are those published previously by Valduga *et al.* (15).

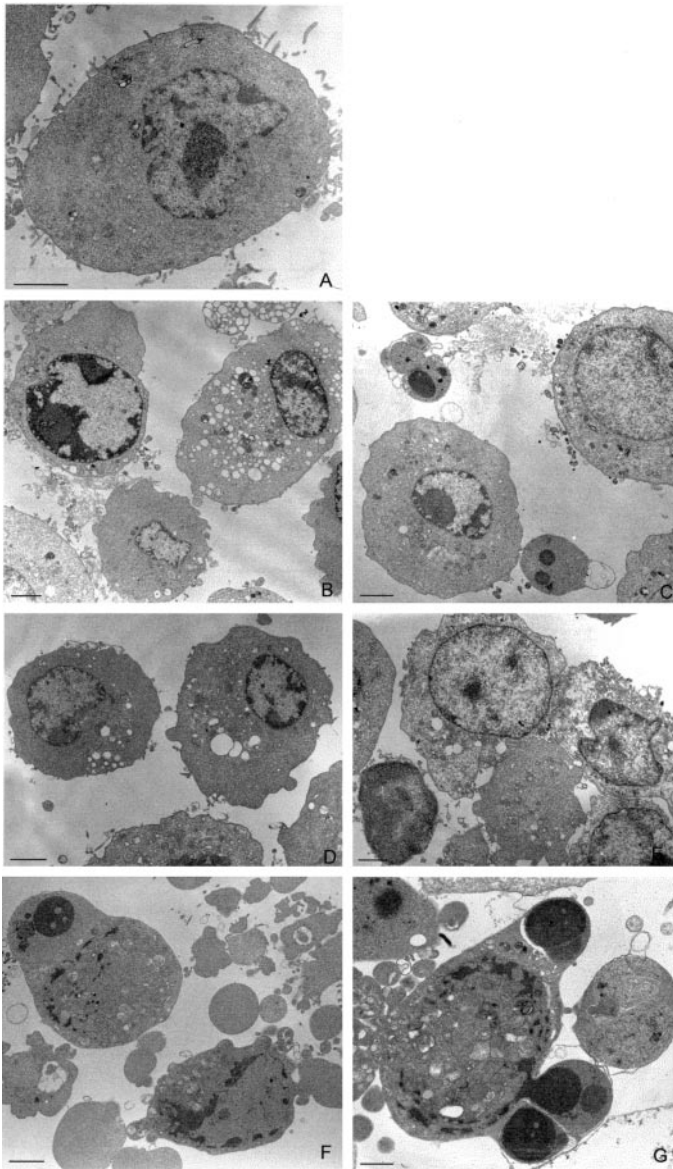


Fig. 6. Morphological alterations induced by ZnPc photosensitization of 4R cells. A, untreated 4R cell after trypsinization. B and C, 4R cells incubated for 2 h with 1  $\mu\text{M}$  of ZnPc and irradiated for 1 min with red light at a fluence rate of 10 mW/cm<sup>2</sup> to reduce cell survival by 50%. At 3 h after PDT (B) some of the damaged cells show chromatin condensation at the periphery of the nucleus, whereas pronounced vacuolization can be observed in others. At 6 h after PDT (C) some apoptotic bodies were found. D and E, 4R cells were incubated for 2 h with 1  $\mu\text{M}$  of ZnPc and irradiated for 3 min with red light at a fluence rate of 10 mW/cm<sup>2</sup> to reduce cell survival by 99.9%. In general, these cells show the presence of large vacuoles at 3 h after treatment (D) and lysis at 6 h (E) as documented by the presence of isolated nuclei. F and G, 4R cells incubated for 24 h with 1  $\mu\text{M}$  of ZnPc and irradiated for 2 min with red light at a fluence rate of 1.5 mW/cm<sup>2</sup> to reduce cell survival by 99.9%. At 3 (F) and 6 h (G) after irradiation the cells show plasma membrane blebbing and extensive fragmentation of the nucleus. Bars = 10  $\mu\text{m}$ .

molecules accumulated in mitochondrial sites remote from the marker enzymes investigated and toward which singlet oxygen or the other reactive species generated during illumination could not easily diffuse. In this connection, Ricchelli *et al.* (26) reported that liposomal ZnPc delivered to isolated rat liver mitochondria localizes mainly in lipid domains of the outer membrane. The lack of direct damage to the major enzyme complexes of the electron transport chain was also observed in a mouse lymphoma cell line treated with PDT with the silicon phthalocyanine Pc4 localized in mitochondria (27). These observations do not exclude the possibility that the higher ZnPc concentration in the mitochondria of cells incubated for 24 compared with 2 h affects the mitochondrial functions differently.

The most striking effect of the incubation time concerns the mechanism of cell death induced by photosensitization with ZnPc. Necrosis represents the prevailing mode of death of cells dark-incubated with ZnPc for 2 h and irradiated with light doses causing >99.9% loss of viability (Fig. 6, D and E). In contrast, cells irradiated after 24-h incubation with ZnPc showed morphological changes typical of apoptosis already at 3 h after PDT (Fig. 6, F and G). In these cells, whereas the whole morphological structure was completely lost, some mitochondria with well-preserved morphology and intact endoplasmic reticulum profile could be observed. The occurrence of the apoptotic process was confirmed by the increased activity of caspase 3 (Fig. 7), which plays a crucial role in the execution phase of apoptosis.

The different mechanism of death in cells irradiated with light doses causing 99.9% mortality after 2- or 24-h incubation is probably determined by several factors. It is well known that apoptosis is an active process that requires ATP for its execution (28). In 4R cells

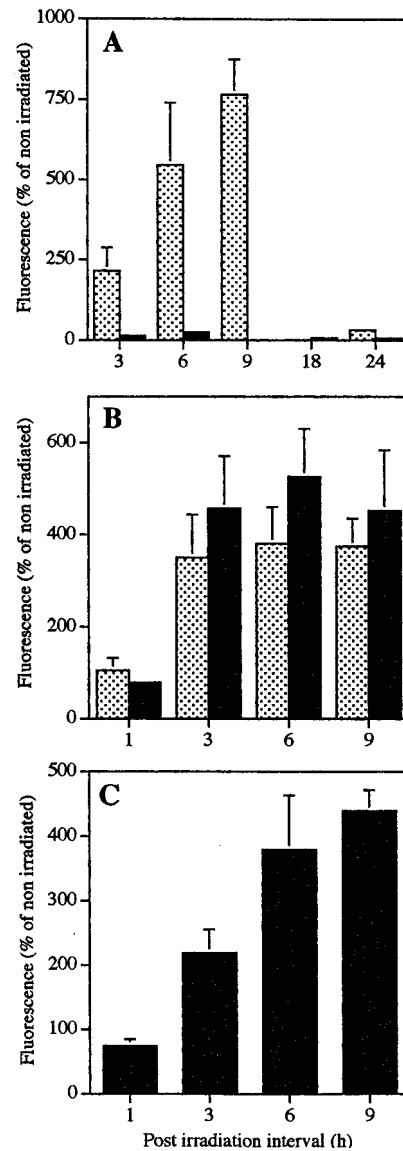


Fig. 7. Activation of caspase 3 in 4R cells at various time periods after PDT treatment with different protocols. A, 4R cells were incubated for 2 h with 1  $\mu\text{M}$  of ZnPc and irradiated for 1 min (▨) or 3 min (■) with light at a fluence rate of 10 mW/cm<sup>2</sup> to reduce cell survival by 50% and 99.9%, respectively; bars,  $\pm$  SE. B, 4R cells were incubated for 24 h with 1  $\mu\text{M}$  of ZnPc and irradiated for 1 min (▨) or 2 min (■) with light at a fluence rate of 1.5 mW/cm<sup>2</sup> to reduce cell survival by 50 and 99.9%, respectively, bars,  $\pm$  SE. C, cells were incubated for 24 h with 0.4  $\mu\text{M}$  of ZnPc and irradiated for 3 min with a fluence rate of 1.5 mW/cm<sup>2</sup> corresponding to 99.9% cell killing; bars,  $\pm$  SE.

receiving a light dose causing 99.9% loss of viability after 2-h incubation, execution of the apoptotic program was prevented by the total depletion of ATP (15). In contrast, in cells irradiated after 24-h incubation with ZnPc, some residual ATP was measured, especially in those photosensitized with 0.4  $\mu\text{M}$  of ZnPc (Fig. 4B). This could be sufficient to allow apoptotic death. The level of ATP in the treated cells probably correlates with inhibition of deoxyglucose transport (Fig. 4, A and B) and, hence, depends at least in part on plasma membrane damage. It has been reported that glycolytic ATP production is more important in tumor cells than in normal cells, probably because of a reduced mitochondrial transmembrane potential (29, 30). We found that 2.5  $\mu\text{M}$  of oligomycin, a blocker of mitochondrial ATP synthesis, reduced the intracellular ATP of 4R cells <40% (data not shown). Thus, it also appears that in this transformed cell line a large fraction of ATP derives from glycolysis and, as a consequence, depends on the availability of glucose. The dose of light used during irradiation may represent an additional parameter determining the mechanism of cell death. The morphological changes and activation of caspase 3 (Fig. 7B) in 4R cells incubated for 2 h and irradiated with a light dose causing only 50% reduction of survival showed the occurrence of both necrosis (Fig. 6B) and apoptosis (Fig. 6C). Under these conditions, the plasma membrane damage was probably less pronounced, and at least one fraction of the dying cells underwent apoptosis before cell lysis occurred.

Our results clearly demonstrate that, at least *in vitro*, it is possible to modulate the mode of ZnPc-sensitized cell death through appropriate choice of experimental protocol. In cells irradiated after short ZnPc incubation, apoptosis is observed only with light doses causing partial reduction of survival, whereas in cells irradiated after long incubation, apoptosis is also observed with light doses causing complete cell mortality. Apoptosis is probably also favored by the low doses of light required for inducing cell death when ZnPc is localized in mitochondria and by the fact that these organelles, not the plasma membrane, are the primary targets of photosensitization. The disruption of mitochondrial membrane functions may be responsible for the apoptotic cell death induced by ZnPc photosensitization. The detailed mechanism will be the subject of additional studies.

The possibility of modulating the mechanism of cell death has great potential in the clinical context. PDT protocols causing necrotic cell death could be applied for treating infiltrating and/or metastatic tumors, where the immune reaction elicited by the inflammatory response to the photoinduced tumor necrosis offers a better control of tumor growth (31). On the other hand, PDT protocols favoring apoptotic cell death may be preferable in cases of *in situ* neoplasia. In these cases, limitation of the inflammatory response is preferred, because matrix-degrading proteases secreted by reactive cells (macrophages and polymorphonucleates) are less available to tumor cells (32). The same protocols will also be of election in cases where rapid tumor mass shrinking is required, as in the case of obstructive bronchus and esophageal cancers (33, 34).

## ACKNOWLEDGMENTS

We thank Dr. S. Biggin for revising the manuscript.

## REFERENCES

- Dougherty, T. J., Gomer, C. J., Henderson, B. W., Jori, G., Kessel, D., Korbek, M., Moan, J., and Peng, Q. Photodynamic therapy. *J. Natl. Cancer Inst.*, 90: 889–905, 1998.
- Trauner, K. B., and Hasan, T. Photodynamic treatment of rheumatoid and inflammatory arthritis. *Photochem. Photobiol.*, 64: 740–750, 1996.
- Levy, J. G., and Obochi, M. New applications in photodynamic therapy. Introduction. *Photochem. Photobiol.*, 64: 737–739, 1996.
- Dougherty, T. J. PDT in the 21<sup>st</sup> Century. *Photodyn. News*, 3: 1–3, 2000.
- Gomer, C. J. Preclinical examination of first and second generation photosensitizers used in photodynamic therapy. *Photochem. Photobiol.*, 54: 1093–1107, 1991.
- Dougherty, T. J. Photodynamic therapy. *Photochem. Photobiol.*, 58: 895–900, 1993.
- Moan, J., and Berg, K. The photodegradation of porphyrins in cells can be used to estimate the lifetime of singlet oxygen. *Photochem. Photobiol.*, 53: 549–553, 1991.
- Kessel, D. Subcellular localization of photosensitizing agents. Introduction. *Photochem. Photobiol.*, 65: 387–388, 1997.
- Oleinick, N. L., and Evans, H. H. The photobiology of photodynamic therapy: cellular targets and mechanisms. *Radiat. Res.*, 150 (Suppl.): s146–s156, 1998.
- Agarwal, M. L., Clay, M. E., Harvey, E. J., Evans, H. H., Antunez, A. R., and Oleinick, N. L. Photodynamic therapy induces rapid cell death by apoptosis in L5178Y mouse lymphoma cells. *Cancer Res.*, 51: 5993–5996, 1991.
- He, X. Y., Sikes, R. A., Thomsen, S., Chung, L. W. K., and Jacques, S. L. Photodynamic therapy with Photofrin II induces programmed cell death in carcinoma cell lines. *Photochem. Photobiol.*, 59: 468–473, 1994.
- Kessel, D., and Luo, Y. Photodynamic therapy: a mitochondrial inducer of apoptosis. *Cell Death Differ.*, 6: 28–35, 1999.
- Schieweck, K., Capraro, H.-G., Isele, U., van Hoogevest, P., Ochsner, M., Maurer, T., and Batt, E. CGP 55847, liposome-delivered zinc(II)-phthalocyanine as a phototherapeutic agent for tumors. In: G. Jori, J. Moan and W. M. Star (eds.), *Photodynamic Therapy of Cancer*, Vol. 2078, pp. 107–118. Bellingham, Washington: SPIE, The International Society for Optical Engineering, 1994.
- Zhou, C., Shunji, C., Jinsheng, D., Junlin, L., Jori, G., and Milanese, C. Apoptosis of mouse MS-2 fibrosarcoma cells induced by photodynamic therapy with Zn(II)-phthalocyanine. *J. Photochem. Photobiol. B Biol.*, 33: 219–223, 1996.
- Valduga, G., Reddi, E., Garbisa, S., and Jori, G. Photosensitization of cells with different metastatic potentials by liposome-delivered Zn(II)-phthalocyanine. *Int. J. Cancer*, 75: 412–417, 1998.
- Rodal, G. H., Rodal, S. K., Moan, J., and Berg, K. Liposome-bound Zn(II)-phthalocyanine. Mechanisms for cellular uptake and photosensitization. *J. Photochem. Photobiol. B Biol.*, 45: 150–159, 1998.
- Valduga, G., Bianco, G., Csik, G., Reddi, E., Masiero, L., Garbisa, S., and Jori, G. Interaction of hydro- or lipophilic phthalocyanines with cells of different metastatic potential. *Biochem. Pharmacol.*, 51: 585–590, 1996.
- Pozzatti, R., Muschel, R., Williams, J., Padmanabhan, R., Howard, B., Liotta, L. A., and Khoury, G. Primary rat embryo cells transformed by one or two oncogenes show different metastatic potential. *Science (Wash. DC)*, 232: 223–227, 1986.
- Garbisa, S., Pozzatti, R., Muschel, R. J., Saffioti, U., Ballin, M., Goldfarb, R. H., Khoury, G., and Liotta, L. A. Secretion of type IV collagenolytic protease and metastatic phenotype: induction by transfection with c-Ha-ras but not c-Ha-ras plus Ad2-E1a. *Cancer Res.*, 47: 1523–1528, 1987.
- Galante, Y. M., and Hatefi, Y. Resolution of complex I and isolation of NADH dehydrogenase and an iron-sulfur protein. In: S. Fleischer and L. Packer (eds.), *Methods in Enzymology*, Vol. 53, pp. 15–21. New York: Academic Press, 1978.
- Reeves, W. J., and Fimognari, G. M. L-lactic dehydrogenase heart (H<sub>2</sub>). In: W. A. Wood (ed.), *Methods in Enzymology*, Vol. 9, pp. 288–294. New York: Academic Press, 1966.
- Beaufay, H., Amar-Costesec, A., Feytmans, E., Thines-Sempoux, D., Wibo, M., Robbi, M., and Berthet, J. Analytical studies of microsomes and isolated subcellular membranes from rat liver. *J. Cell Biol.*, 61: 188–200, 1974.
- Smith, P. K., Krohn, R. L., Hermanson, G. T., Mallia, A. K., Gartner, F. H., Provenzano, M. D., Fujimoto, E. K., Goeke, N. M., Olson, B. J., and Klenk, D. C. Measurement of protein using bicinchoninic acid. *Anal. Biochem.*, 150: 76–85, 1985.
- Brandli, A. W., Hansson, G. C., Rodriguez-Boulan, E., and Simons, K. A polarized epithelial cell mutant deficient in translocation of UDP-galactose into the Golgi complex. *J. Biol. Chem.*, 263: 16283–16290, 1988.
- Moan, J., McGhie, J., and Jacobsen, P. B. Photodynamic effects on cells *in vitro* exposed to hematoporphyrin derivative and light. *Photochem. Photobiol.*, 37: 599–604, 1983.
- Riccihelli, F., Nikolov, P., Gobbo, S., Jori, G., Moreno, G., and Salet, C. Interaction of phthalocyanines with lipid membranes: a spectroscopic and functional study on isolated rat liver mitochondria. *Biochim. Biophys. Acta*, 1196: 165–171, 1994.
- Varnes, M. E., Chiu, S.-M., Xue, L.-Y., and Oleinick, N. L. Photodynamic therapy-induced apoptosis in lymphoma cells: translocation of cytochrome c causes inhibition of respiration as well as caspase activation. *Biochem. Biophys. Res. Commun.*, 255: 673–679, 1999.
- Leist, M., Single, B., Castoldi, A. F., Kühnle, S., and Nicotera, P. Intracellular adenosine triphosphate (ATP) concentration: a switch in the decision between apoptosis and necrosis. *J. Exp. Med.*, 185: 1481–1486, 1997.
- Burk, D., Woods, M., and Hunter, J. On the significance of glycolysis for cancer growth, with specific reference to Morris rat hepatomas. *J. Natl. Cancer Inst.*, 38: 839–863, 1967.
- Johnson, L. V., Summerhayes, I. C., and Chen, L. B. Decreased uptake and retention of rhodamine 123 by mitochondria in feline sarcoma virus-transformed mink cells. *Cell*, 28: 7–14, 1982.
- Korbek, M. Induction of tumor immunity by photodynamic therapy. *J. Clin. Laser Med. Surg.*, 14: 329–334, 1996.
- Sternlicht, M. D., and Werb, Z. Matrix metalloproteinases (MMPs). In: T. Kreis and R. Vale (eds.), *Extracellular Matrix, Anchor, and Adhesion Proteins*, pp. 519–524. Oxford, United Kingdom: University Press, 1999.
- Lightdale, C. J., Heier, S. K., Marcon, N. E., McCoughan, J. S., Jr., Gerdes, H., Overholt, B. F., Sivak, M. V., Jr., Stiegmann, G. V., and Nava, H. R. Photodynamic therapy with porfimer sodium *versus* thermal ablation therapy with Nd:YAG laser for palliation of esophageal cancer: a multicenter randomized trial. *Gastrointest. Endosc.*, 42: 507–512, 1995.
- Lam, S., Crofton, C., and Cory, P. Combined Photodynamic Therapy (PDT) using Photofrin and radiotherapy (XRT) *versus* radiotherapy alone in patients with inoperable distribution non-small cell bronchogenic cancer. *Proc. SPIE*, 20–28: 1991.